

# **Multi-modal Optimization of Offshore Wind Farm Collection System Topology Based on Nearest Better Most Attractive Particle Swarm Optimization**

Yuchen Wang<sup>1</sup>, Dongran Song<sup>1,\*</sup>, Filip Jurić<sup>2</sup>, Neven Duić<sup>2</sup>, Hrvoje Mikulčić<sup>2,\*</sup>

<sup>1</sup>School of Automation, Central South University, Changsha, China

<sup>2</sup>Faculty of Mechanical Engineering and Naval Architecture, University of  
Zagreb, Croatia

**Abstract:** The offshore wind farm collection system plays a crucial role in the development of offshore wind farms, reducing their significant construction costs as a key area of research. In complex and uncertain marine environments, solving strategies based on unique global optimization often fail to meet engineering design needs. This paper proposes an innovative solution for multi-modal optimization of the offshore wind farm collection system topology that provides designers with more decision-making freedom. In terms of the goal of minimizing cost, this research comprehensively considers capital cable costs, cable installation, and energy loss, taking into account the uncertainty of wind conditions. Additionally, the research combines the Weibull distribution model and the Jensen wake model to calculate the wind distribution. In terms of the optimization algorithm, a novel multi-modal algorithm, named Nearest Better Most Attractive Particle Swarm Optimization (NBMA-PSO), is proposed, in which the Prim algorithm is employed for population initialization, subpopulation grouping is achieved through a normalized difference representation and population balance strategy, and the iterative optimization is implemented through a two-stage PSO algorithm. Case analysis shows that compared with existing optimization algorithms, the proposed NBMA-PSO algorithm has better solving efficiency and stability and can effectively obtain multi-modal solutions. The proposed NBMA-PSO algorithm efficiently balances exploration and exploitation in offshore wind farm collection system optimization, demonstrating its capability to generate multiple high-quality solutions while reducing total costs by up to 4.1% compared to traditional counterparts.

**Keywords:** Offshore wind farm; Collection system Topology; Multi-modal algorithm; NBMA-PSO

**\* Co-Correspondence**

Dongran Song, email: [songdongran@csu.edu.cn](mailto:songdongran@csu.edu.cn)

Hrvoje Mikulčić, email: [hrvoje.mikulcic@fsb.unizg.hr](mailto:hrvoje.mikulcic@fsb.unizg.hr)

# **1. Introduction**

In this section, the research background is firstly introduced. Then, the literature review is performed. Following that, the contribution and organization of the work are given.

## **1.1. Background**

As the global economy rapidly evolves, there has been a significant surge in both industrial production and residential living standards, consequently driving an escalating energy demand [1]. In contrast, the excessive exploitation of global non-renewable energy sources has led to significant challenges, including climate warming. There is an urgent need to develop green, clean, and abundant renewable energy sources, prompting nations to substantially increase their investment in renewable energy research [2]. Wind power, with its plentiful resources and clean energy attributes, is acknowledged by both the academic and industrial sectors as the most mature, extensively utilized, and promising renewable energy technology [3]. Compared to onshore wind energy, offshore wind energy offers several benefits, such as the absence of land resource consumption, longer annual operational hours, minimal interference with other infrastructure, and abundant wind energy potential. However, the growth of offshore wind farms has been hindered by the challenges related to construction and maintenance, as well as the increased operational costs.

In offshore wind farms, the power collection system manages the power generated and transmits it to the grid for grid connection via submarine cables. Its reliability is crucial to ensure the smooth operation of offshore wind farms. Usually, the investment cost of the power collection system accounts for about 15% to 30% of the total investment cost of an offshore wind farm [4]. This percentage may further increase as the size and distance of offshore wind farms increase. In order to reduce the levelized cost of electricity (LCOE) of offshore wind power, it is crucial to optimize the topology design of the power collection system because it directly affects the power generation efficiency of offshore wind power. However, offshore wind farms face many challenges, such as salt spray corrosion, navigational requirements, typhoons, and complex

undersea environments, which make the design of their power collection systems much more complex than that of onshore wind farms [5][6].

## **1.2. Literature review**

The collection system topology is related to the voltage level. Related to the voltage level, there are two types of topology: AC collection systems and DC collection systems. Starting from this point, this section provides a review of existing research on collection systems, optimization algorithms, and multimodal algorithms.

### *1.2.1 Collection System Topology*

There are notable differences in both the economic performance and reliability of various collector system topologies. The reliability and cost-effectiveness of a system under different topological configurations can be evaluated using methods such as block enumeration and minimal path approaches, with consideration given to the failure rates of electrical components. Among commonly implemented collector system topologies, the single-sided ring topology demonstrates the highest reliability in offshore wind farm applications [7,8]. For long-distance, large-capacity offshore wind farms, the double-sided toroidal collector system topology offers substantial advantages by achieving an effective balance between economics and reliability [9,10]. Although the chain topology is often favored for its economic efficiency, implementing a well-designed switch configuration can also result in satisfactory reliability levels [11]. Particularly for the ring topology, which is widely adopted in offshore wind farms to ensure high reliability, the availability rate can be quantitatively assessed using fault tree analysis that integrates both probabilistic and deterministic approaches. This provides a basis for metrics-driven reliability assessment [12], enabling the optimization of system elements such as the switch configuration under the ring topology and ultimately yielding further improvements in overall system stability [13].

Generally, the high-voltage direct current (HVDC) scheme is comparable to the high-voltage alternating current (HVAC) scheme in terms of construction costs for long-distance transmission, but it offers lower losses and superior performance, which can significantly enhance the economic benefits of long-distance offshore wind farms

[14-16]. The advancement of HVDC technology has enabled the integration of large-capacity offshore wind turbines with DC transmission systems. As a result, the economic efficiency and reliability of delivering wind power to onshore grids via DC lines are substantially improved [17]. At present, all HVDC transmission solutions for offshore wind farms utilize flexible DC technology.

The 35 kV AC collection system not only suffers from inherent limitations, such as low transmission capacity but also necessitates the construction of additional offshore booster stations when combined with 66 kV HVDC transmission systems. Therefore, the 66 kV AC collection system is a more advantageous option. In the 66 kV DC collection system design employing high-voltage flexible DC transmission, as proposed by European TenneT, the offshore booster station is omitted, allowing direct connection of 66 kV wind turbines to the offshore converter station for power transmission [18]. Although operational data for 66 kV wind turbines remains limited and the elimination of booster stations increases the number of feeder circuits connected to offshore converter stations (and GIS equipment thus occupies more space), this configuration enables the use of submarine cables with smaller cross-sectional areas for the same transmission capacity, leading to significant reductions in investment costs. Downsizing the offshore converter station further lessens submarine cable expenditure and construction costs, and enables savings on transformer and auxiliary transformer investments. The increased voltage level also reduces system losses, eases maintenance, and ultimately lowers the overall construction investment for offshore wind farm collection systems [19,20].

However, this integrated solution requires multiple rectification and inversion stages and places stringent demands on equipment specifications. Research indicates that the integration of DC collection systems with DC transmission systems can greatly simplify power delivery processes and reduce system losses [21]. It is foreseeable that, as DC collection and flexible DC transmission technologies continue to advance, this approach will gradually become the mainstream solution for deep-sea power collection and transmission [22]. This will further decrease the investment costs of deep-sea wind farm collection systems while substantially enhancing system reliability.

Offshore wind farm DC collector system topologies mainly include series, parallel, series-parallel, and matrix interconnections [23,24]. Additionally, a new radial DC collector system topology, which is particularly suitable for scenarios where wind turbine generators (WTGs) are irregularly arranged, has been widely studied [25]. However, its economic performance and reliability require further investigation.

Compared with AC collector schemes, DC collector schemes can significantly reduce the cost of constructing the collector system [26,27]. However, DC collector systems require components such as DC circuit breakers, DC wind turbines, and DC/DC converters, which are not yet technologically mature, especially for offshore wind farms where operation and maintenance are more challenging. As a result, there are currently no commercially operated DC collector systems.

### *1.2.2 Collection System Topology Optimization*

The algorithms used to solve topology optimization problems in offshore wind farm collection systems in existing studies generally fall into two categories. The first category encompasses deterministic algorithms, such as the minimum spanning tree (MST) algorithm based on graph theory, which produces consistent outputs given consistent inputs. For example, Li et al. [28] accounted for restricted regions and employed Delaunay triangulation along with the MST algorithm to optimize cable routing. Huang et al. [29] integrated GIS techniques with obstacle avoidance algorithms to enhance the effectiveness of path optimization. Shen et al. [30] utilized mixed integer linear programming (MILP) to minimize both cable investment costs and power losses. Chen et al. [31] adopted simulated annealing (SA) algorithms to improve the grouping and configuration of cable topology, thereby enhancing overall optimization and efficiency. Zuo et al. [32] developed a mixed-integer programming algorithm for the comprehensive joint optimization of offshore wind farm planning. X. Shen et al. [33] employed a mixed integer quadratic programming (MIQP) algorithm with an “N-1” criterion to optimize the dual-ring topology of the offshore wind farm collection system, thereby enhancing system reliability and economic performance. Furthermore, Chen et al. [34] combined fuzzy C-means (FCM) clustering and binary integer programming

(BIP) for network model generation and automated wind turbine allocation. Li et al. [35] integrated FCM with Delaunay triangulation using dynamic edge weights, catering to the complexities of collector system topology optimization. Although deterministic algorithms are widely applied to this type of topology optimization problem, they are prone to becoming trapped in local optima.

Another category encompasses heuristic algorithms, exemplified by the particle swarm optimization (PSO) algorithm. Within the field of heuristic algorithm applications, Gonzalez et al. [36] proposed optimizing power pooling system topology by combining a Genetic Algorithm with the Multi-Travelling Salesman Problem (MTSP). Zhao et al. [37] utilized an improved Genetic Algorithm to enhance both the economic efficiency and reliability of offshore wind farm power pooling system topologies. Song et al. [38] introduced a hybrid optimization framework that integrates Binary Particle Swarm Optimization (BPSO) with Improved Monte Carlo Tree Search (IMCTS), considering specific floating characteristics and influencing factors. Wei et al. **Error! Reference source not found.** addressed the high-dimensionality problem in large-scale wind farms by employing a fuzzy clustering algorithm, a Single-Parent Genetic Algorithm (SPGA), and an MTSP model. Srikakulapu et al. [39] combined Ant Colony Optimization (ACO) with the MTSP to optimize collection system topology. Zuo et al. [40] presented a two-tier optimization framework that incorporates Deterministic Fuzzy C-Means clustering and a Genetic Algorithm (GA), balancing economic efficiency with output stability. Wu et al. [41] improved planning efficiency and optimality by coupling an enhanced fuzzy C-Means clustering algorithm (FCM) with Prim's algorithm. Liu et al. [42] increased search efficiency by reducing problem size through a partitioning strategy. Wang et al. [43] proposed an improved Genetic Algorithm to enhance optimality search and convergence, making it suitable for collector system topology optimization. These algorithms offer greater flexibility and the potential to identify global optimal solutions, but their outputs are random and unstable. In a recent study, Zhang et al [44] assisted in the clustering of turbine clusters based on a large language model (LLM), which enabled the LLM to understand the optimization objective through the chain cueing method, and used the LLM to partition

the large-scale offshore wind farm into several small regions to reduce the dimensionality of the optimization problem and to improve the speed and quality of the solution.

While the above studies provide a globally optimal solution for the collection system topology design problem, the multimodal nature of the problem has not been explored. Since the collection system topology presents a high-dimensional optimization problem, the problem should have multiple optimal solutions simultaneously. Multimodal algorithms provide a solution to this need. Unlike multi-objective algorithms, multimodal algorithms focus on finding solutions on different Pareto frontiers. This means that multimodal algorithms can find multiple solutions that are not identical while satisfying the optimization objective. As shown in Figure 1, the left side is the decision space, and the right side is the objective space. The two curves PS1 and PS2 in the decision space represent solution sets, and the feasible solutions A1 and A2, although separated by a distance  $d_1$  in the decision space, are both mapped to point A in the objective space. In the design of the collection system, the multimodal characteristic is particularly pronounced. For instance, employing submarine cables with a larger cross-sectional area, while incurring a higher investment cost for the cables, may reduce the loss costs, thereby achieving a comparable total investment expenditure.

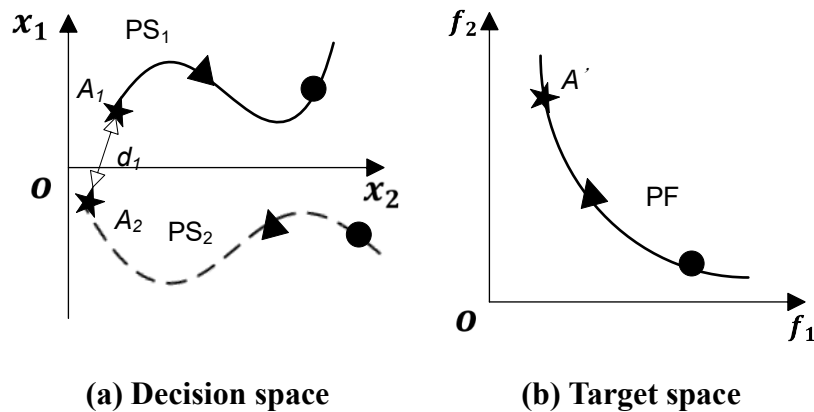


**Figure 1** Schematic diagram of multimodal optimization

### 1.2.3 Multimodal Optimal Algorithms

Existing multimodal algorithms can be roughly divided into two categories. One does not explicitly divide the subpopulations, but takes the distance between solutions

as the optimization objective and solves it with the help of the idea of multi-objective algorithms. However, this category of methods is ineffective in coping with high-dimensional complex problems. The other involves the neighborhood topology strategy, which explicitly divides the subpopulations. Therein, the niche strategy is widely adopted. Niching optimization is a set of optimization schemes that aims to enhance general-purpose metaheuristics and help them identify multiple local optima simultaneously [45]-[47]. Specifically, by introducing the concept of niches from biology, individuals in the population evolve in different specific living environments, thereby searching the entire solution space to find more global or local optimal solutions [48]. Niching techniques were introduced to maintain diversity within metaheuristic algorithms, which are typically unimodal and tend to converge toward a single promising region. Niching approaches can be broadly classified into three categories: sequential or temporal niching, parallel or spatial niching, and hybrid niching methods. These techniques have been employed to enhance the exploratory capabilities of major metaheuristics, including genetic algorithms [49], particle swarm optimization [50], differential evolution [51], and ant colony optimization [52], as well as more recent algorithms such as the bat algorithm [53], chimp optimization [54], whale optimization [55], and harmony search optimization [56]. Among them, combining the niching technique with the particle swarm algorithm gives good results for solving nonlinear problems. Niche-PSO [57] and Species-PSO [58] algorithms are two commonly used multimodal algorithms based on PSO algorithms and improved niching techniques. The Omni-optimizer algorithm is another commonly used multimodal algorithm, in which the environmental selection mechanism ranks and allocates individuals based on three indicators: non-dominated sorting, decision space crowding distance, and objective space crowding distance [59]. Shi et al. [60] proposed the MMOEA-GD algorithm, which uses the harmonic average distance in the decision space to measure the neighborhood relationship of the population in the decision space, thereby improving the diversity of solutions in the decision space. Nevertheless, to the best of the authors' knowledge, studies employing multimodal algorithms to solve topology optimization problems are lacking.

### 1.3. Research gap and contribution

In [61], the authors applied a multimodal algorithm named Nearest Better Neighbor Clustering-Particle Swarm Optimization (NBNC-PSO) to the topology optimization of offshore wind farm collection systems for the first time. Therein, the effectiveness of multimodal algorithms was confirmed, but three key challenges remain to be solved:

- How to accurately characterize the distance between solutions in the objective space and decision space. In the context of offshore wind farm collection systems, the complexity is heightened by the presence of numerous variables, encompassing continuous, discrete, and interrelated types, which complicates the representation of solution distances within the decision space.
- How to reasonably divide the population size to obtain a high-quality modal number. The solution space for the topology optimization of offshore wind farm collection systems typically exhibits multiple peaks, yet the majority of these solutions fail to align with the criteria of economic viability and reliability. An overly large subpopulation size may lead to convergence on suboptimal solutions, thereby squandering computational resources. It is crucial to partition the population judiciously to avoid an excessive or insufficient number of modalities.
- How to achieve an effective balance between exploration and exploitation during the optimization process. To achieve a greater variety of solutions, the algorithm must preserve the diversity of solutions, striving to explore a larger target space while also focusing on local optimization. The solutions should be closely clustered in the target space but widely dispersed in the decision space. This necessitates a judicious grouping of solutions that maintains robust search capabilities, ensuring the quality of solutions within a confined area and preventing premature convergence.

Motivated by the above observations and discussions, this work aims to propose a multimodal algorithm for the topology optimization of offshore wind farm collection systems. With regard to the literature, the main contributions of this work can be stated as follows: Firstly, the importance and necessity of multimodal optimization in offshore

wind farm collection system topology design are explained in detail. Secondly, this paper proposes a new multimodal algorithm, named Nearest Better Most Attractive Particle Swarm Optimization (NBMA-PSO), which is suitable for complex problems with a mixture of discrete and continuous variables. Thirdly, the NBMA-PSO is validated both on the test functions and the collection system of a real wind farm. Finally, this paper explains how decision makers can design based on the multimodal solution.

It is worth noting that the concept and application of attractiveness are the core of the NBMA-PSO algorithm, distinguishes it from existing multimodal optimization algorithms. Existing algorithms usually divide the niches only by the distance between the optimal individual of the subpopulation and the other individuals, and enforce the evolutionary direction for each particle from the overall perspective, such as MMOEA-GD [60] and NBNC-PSO [61]. Such methods somewhat ignore the individual randomness of particles and require additional clustering algorithms or complex small habitat radius constraints to maintain diversity. For the proposed NBMA-PSO algorithm, the attractiveness is calculated so that the attractiveness between each individual is fully considered in the generation of the niche. Different from the existing deterministic approach to niche division, this paper proposes a guided approach to niche generation, which divides the niche based on the optimization direction selection of each individual, greatly improving the flexibility of the algorithm. This ensures that the algorithm has a good global search capability. Meanwhile, the calculation of attractiveness causes niche generation to be influenced by both the degree of difference and the fitness value simultaneously. Instead of selecting the nearest subpopulation, this allows the particle to improve its judgment of the solution's quality, enabling the algorithm to naturally filter out poorer peaks. Such an approach allows the algorithm to reduce arithmetic requirements by eliminating the need for additional elite solution judgment strategies.

Table 1 compares the available algorithms in the literature, including those relating to the topology optimization of offshore wind farm collector systems and multimodal

algorithms. The various algorithms differ in terms of their type, their focus, and how they handle constraints.

**Table 1 Overview of offshore wind farm collection system and multimodal algorithm studies**

Ref	Year	Multi-modal	Algorithm Type	Constraint Handling	Research Focus
[30]	2021	×	MILP	Exact	Large-scale planning
[31]	2024	×	ISA	Heuristic	Topology optimization
[32]	2024	×	Joint Optimization	Heuristic	Comprehensive optimization
[33]	2023	×	MILP	Exact	Double-sided ring planning
[37]	2019	×	Improved Genetic Algorithm	Heuristic	Topology structure optimization
[38]	2023	×	Hybrid Method	Hybrid	Floating wind farm
[40]	2021	×	Hybrid Method	Hybrid	Large-scale planning
[42]	2023	×	Divide and Conquer Strategy	Heuristic	Topology optimization
[44]	2024	×	Large Language Model	Hybrid	Large-scale planning
[48]	2022	√	Hierarchy Rank	Heuristic	Multi-objective optimization
[59]	2025	√	Hierarchical Cluster	Heuristic	Hierarchical clustering algorithm
[60]	2019	√	Density Update	Heuristic	Multi-objective optimization

[61]	2024	√	Niching	Heuristic	Collector system optimization
This Paper	2025	√	Improved niching	Heuristic	High-dimensional multimodal optimization

The remaining sections are arranged as follows: Section 2 provides a detailed explanation of the necessity of multimodal optimization for the offshore wind farm collection system topology, highlighting the need for its engineering application. Section 3 presents the methodology used in this study, including the optimization problem modeling and the proposed multimodal algorithm. Section 4 presents the optimization results of the proposed algorithm on standard CEC multi-peak test functions. After that, Section 5 examines a wind farm case study to demonstrate the usefulness and feasibility of the proposed method in practical engineering applications. The limitations of the study and how decision makers can use the multimodal solutions derived from the algorithm for wind farm collection system planning are also described. Finally, Section 6 concludes the study.

## 2. Necessity for multimodal optimization

Since the collection system of offshore wind farms is less affected by the topography and has numerous cable routing paths, schemes with the same total cost but different topological connections exist. As shown in Figure 2, the two topologies of the collection system correspond to the same cable length, total cost, and number of nodes, but they feature different connections.

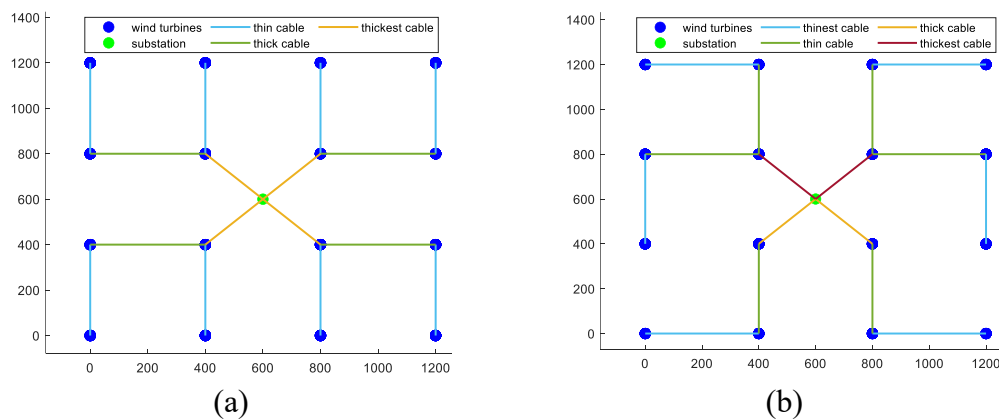


Figure 2 Two topologies with the same total cost but different structures

In existing research, single-modal algorithms originally designed for the optimization of power collection systems for onshore wind farms have been widely used in the optimization of offshore wind farm systems. Due to the numerous constraints of onshore wind farms, such as terrain and transportation, there are limited options available for the topology of the power collection system, and the need for multimodality is not obvious. However, in marine environments with uncertainties, a single optimal topology solution often cannot achieve the expected results in actual construction, which requires designers to provide decision makers with multiple feasible solutions to choose from.

In addition, existing research methods primarily employ topology optimization with a fixed wind direction and do not account for the impact of varying wind directions on the cost of the collector system. As a result, the optimal solution identified using unimodal algorithms may not yield the lowest cost if the wind direction changes even slightly. Accurately modeling the cost variation as a function of wind direction using explicit equations is challenging, and incorporating this consideration directly into the optimization objective would lead to a substantial increase in computational cost. By contrast, multimodal algorithms can provide multiple candidate solutions. By analyzing the cost variations of these multimodal solutions under different wind directions, it becomes feasible to select the solution with the lowest cost for any given wind direction. This approach avoids the need to explicitly consider wind direction changes during the optimization process, thereby significantly reducing computational costs. Due to the large number of uncertainties in real engineering, multimodal solving greatly improves the flexibility of design.

### **3. Methodology**

This section describes in detail the full life cycle cost model of the offshore wind farm collection system and the proposed NBMA-PSO multimodal algorithm. The general content is shown in Figure 3.

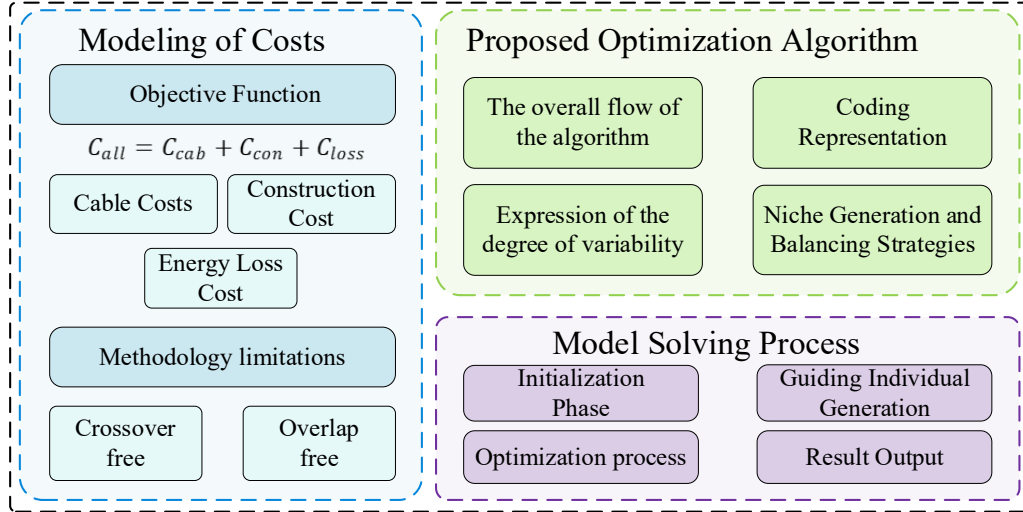


**Figure 3** Block diagram of the main elements of the model and algorithm

### 3.1. Modeling of Costs

In the majority of studies, the objective of optimizing the topology of the collection system is to minimize the cable length, thereby reducing the total distance of cable connections between wind turbines and between wind turbines and the substation to the shortest possible extent. In practice, when considering the reduction of cable investment costs, it is equally important to select the cable model and consider the cost incurred by system operation losses. To achieve a balance between the long-term operational loss cost of a wind farm and the investment cost associated with cable layout, this paper identifies cable connections, cable types, and substation locations as optimization variables. It integrates the Jensen wake model and takes into account cable investment costs, construction costs, and energy loss costs to develop a comprehensive total cost model for the topology optimization of the collection system. The uncertainty of wind turbine output mainly stems from the inherent intermittency, randomness, and volatility of wind speed. The academic and industrial communities generally agree that the probability distribution of wind speed follows the classical two-parameter Weibull distribution. This paper uses the Weibull distribution to represent wind speed, thereby enhancing the robustness of the model.

#### 3.1.1 Objective Function

The total topology cost of the offshore wind farm collection system  $C_{all}$  includes capital cable costs, cable installation, and energy loss, which can be expressed as:

$$C_{all} = C_{cab} + C_{con} + C_{loss} \quad (1)$$

The cable investment cost,  $C_{cab}$ , refers to the purchase price of submarine cables within this system.  $C_{cab}$  is determined by the length and model of the submarine cables and constitutes a significant portion of the investment in the collection system topology optimization. By optimizing the cable connection topology, this cost can be significantly reduced. The construction cost  $C_{con}$  refers to the construction price required for laying submarine cables, and its magnitude is only related to the length of the submarine cables. The energy loss cost  $C_{loss}$  refers to the electricity price corresponding to the energy dissipation in the submarine cables. During the operation of the wind farm, its magnitude is primarily determined by the current through each cable.

The cable investment cost  $C_{cab}$  can be expressed as:

$$C_{cab} = 3 \sum_{i=1}^{N_{cab}} X_i Z_i \quad (2)$$

where  $N_{cab}$  represents the total number of submarine cable segments,  $X_i$  denotes the length of the  $i^{\text{th}}$  cable segment, and  $Z_i$  indicates the unit length price of the single-phase cable model corresponding to the  $i^{\text{th}}$  segment.

The construction cost  $C_{con}$  can be expressed as:

$$C_{con} = w \sum_{i=1}^{N_{cab}} X_i \quad (3)$$

where  $w$  represents the cost per unit length for the construction of submarine cables. According to the literature [62], the cost per unit length for the construction of submarine cables in engineering can be defined or set  $w = 8000$  PLN/km, and converted according to the exchange rate  $1\text{PLN} = 1.4899$  CNY(RMB).

The energy loss cost  $C_{loss}$  can be expressed as:

$$C_{loss} = 3 \sum_{k=1}^{K_n} \sum_{t=1}^T \sum_{i=1}^{N_{cab}} \frac{e_t}{(1+r)^t} I_{i,k}^2 R_i X_i (8760 p_k) \quad (4)$$

where  $K_n$  represents the total number of different wind conditions that occurred in the current year,  $T$  represents the total number of years the wind farm has been in operation,  $e_t$  represents the electricity price in the  $t$ -th year,  $r$  represents the inflation

rate,  $R_i$  represents the unit length resistance corresponding to the single-phase cable model in the section  $i$ ,  $p_k$  represents the probability that the number of hours the wind condition  $k$  appeared in the current year accounts for the total number of hours in the year,  $I_{i,k}$  represents the current flowing through the cable in the section  $i$  under the wind condition  $k$  in the current year, calculated as follows:

$$I_{i,k} = \frac{P_i}{\sqrt{3} \cos\varphi U_n} \quad (5)$$

where  $U_n$  represents the operating voltage of the wind turbine under rated conditions,  $\cos\varphi$  represents the power factor of wind turbine generation, and  $P_i$  represents the total power generation of wind turbines connecting to the cable  $i$  and is calculated by

$$P_i = n f^{std} f(v; c, k) \quad (6)$$

where  $n$  represents the number of wind turbines connecting to the cable  $i$ ,  $f^{std}$  represents the standard wind speed-power curve of the wind turbine, and  $f(v; c, k)$  represents the Weibull distribution function of wind speed [633,64].

$$f(v; c, k) = \left(\frac{k}{c}\right) \left(\frac{v}{c}\right)^{k-1} \exp \left[-\left(\frac{v}{c}\right)^k\right] \quad (7)$$

where  $v$  represents the actual wind speed,  $c$  is the scale parameter, which magnifies or reduces the curve but does not affect the shape of the distribution.  $k$  is the shape parameter, which determines the basic shape of the distribution density curve.

As the scale of offshore wind farms continues to grow, the impact of wake effects is intensifying. To accurately ascertain the power output of each wind turbine, this study adopts the Jensen model, widely recognized in engineering applications and particularly suited for extended operational analyses of offshore wind farms [655,66]. By employing this model, the actual power generation of the wind turbines is simulated to increase the accuracy of energy loss cost calculations.

### 3.1.2 Methodology limitations

For the connection between different wind turbines, based on the minimum spanning tree principle, the following constraints are made.

$$F_i \bigcap_{\substack{i,j \in S \\ i \neq j}} F_j = \emptyset \quad (8)$$

$$F_i \cup F_j = S \quad (9)$$

where  $F_i$  and  $F_j$  represent the  $i$ th and  $j$ th wind turbines, respectively, and  $S$  represents the set of all wind turbines. The constraint condition indicates that there can be no intersection between wind turbine groups, and all wind turbines must be included in the wind turbine set  $S$ .

Considering that cable crossings and overlaps greatly increase the probability of failures in the offshore wind farm electrical system, the constraint is set to avoid cable crossings and overlaps in the collection system topology as follows.

$$i \bigcap_{i \neq j} j \neq \emptyset \quad \forall i, j \in \{1, 2, \dots, N_{cab}\} \quad (10)$$

where  $i$  and  $j$  are two separate cables that are positioned in the cable concentration, and the intersection is an empty set, meaning that cables will not cross or overlap.

In practical algorithm design, cable crossings are identified when the intersection point of the corresponding lines of two cables lies on the cable segment itself, whereas cable overlaps are recognized when the slopes of the corresponding lines of two cables are identical. The algorithm sets penalty terms to make the fitness value for such cases very large, thereby avoiding these situations.

### 3.2. Proposed Optimization Algorithm

The NBMA-PSO algorithm proposed herein incorporates the concept of niche strategy, which hinges on two pivotal factors: the establishment of a suitable niche framework that leverages the discrete nature of the model, and the selection of an optimization algorithm celebrated for its robust search capabilities. As illustrated in Figure 4, the algorithm architecture is primarily divided into three components: the encoding of optimization variables and dissimilarity representation, a niche grouping strategy based on dissimilarity, and an iterative solution for individual evolution strategies grounded in PSO.

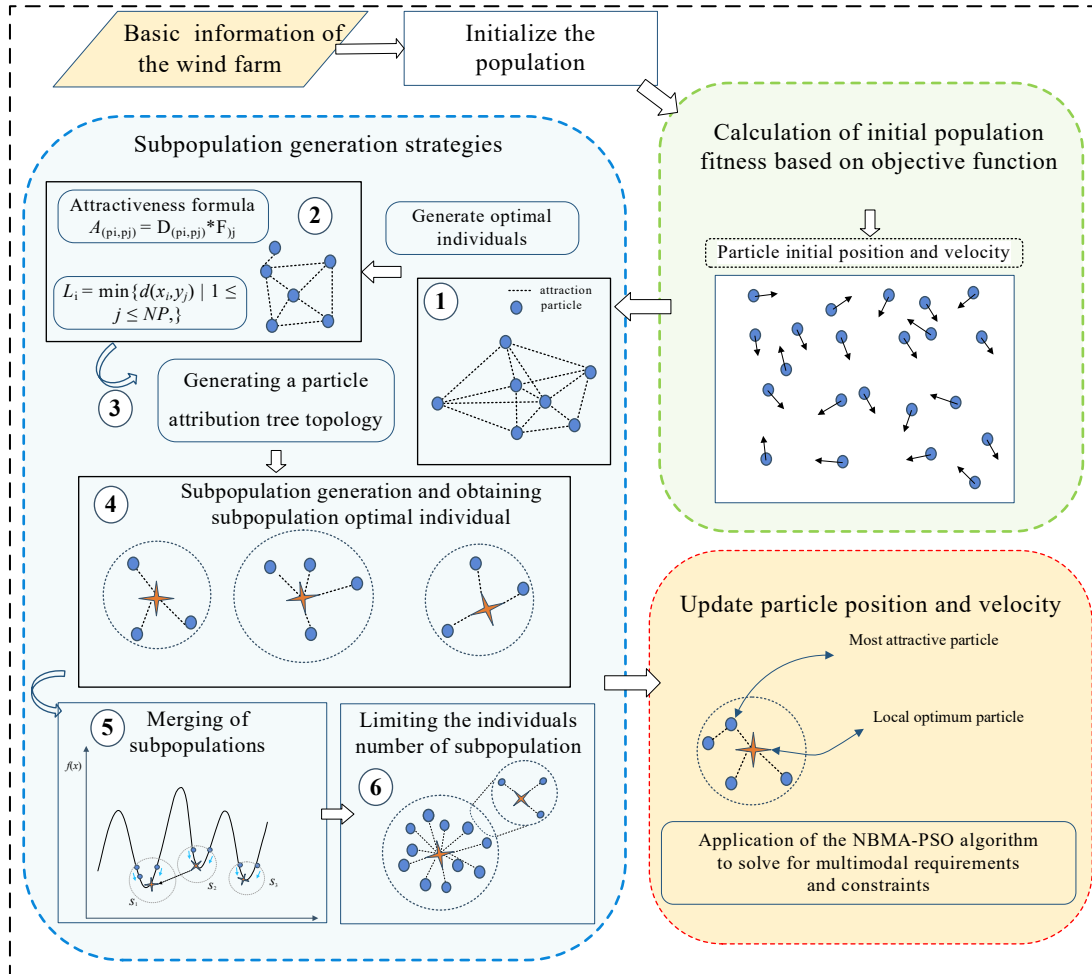


**Figure 4 Framework of Proposed NBMA-PSO Algorithm**

As shown in Table 2, the main difference between the proposed algorithm and the baseline PSO algorithm is the generation of sub-populations and particle update guidance. The goal of classical PSO is to find a globally optimal solution so that all particles take the globally optimal position as the direction of evolution. In contrast, the algorithm matches the most attractive individual and the locally optimal individual for each particle through the NBMA strategy. The formula of the particle velocity update no longer contains the global optimal position, but replaces it with the position of the most attractive individual or the local optimal individual. This greatly improves the global search ability of the algorithm and makes the algorithm capable of multimodal search.

**Table 2 Difference between NBMA-PSO and baseline PSO**

Comparison Dimension	Baseline PSO	NBMA-PSO
----------------------	--------------	----------

Number of solutions	Single	Multiple
Population structure	Single global population	Multiple sub-populations derived from dynamic species delimitation
Particle position update guidance mechanism	Fixed guidance with gbest and lbest	Dynamic species center guidance based on attractiveness
Mechanisms for diversity maintenance	No dedicated mechanism	Niche generation + Population merging mechanism

### 3.2.1. Coding Representation

It is required to accurately encode the variables in each dimension, which is the basis for intelligent algorithmic solutions, in order to correctly characterize the distance of different solutions in the decision space. For the three dimensions of the collection system, this paper represents them as individual vectors by hybrid coding, as shown in Figure 5.

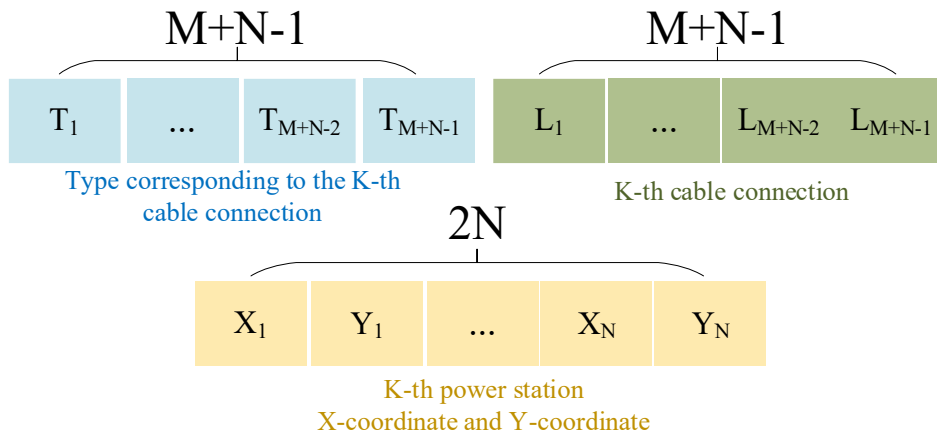


**Figure 5 Schematic Diagram of Optimized Variable Encoding**

Assuming the collection system comprises  $M$  wind turbines and  $N$  substations, the algorithm rules presented are as follows: The individual location dimension consists of three key components: the coordinate information of the  $x$  and  $y$  axes of the  $N$  substations,  $M+N-1$  cable connections, and the cable models corresponding to these  $M+N-1$  connections. For the location of substations, their  $x$  and  $y$  coordinates are usually selected within the boundaries of the given range, i.e., the limits of each dimension in the first part are the boundary range of the whole offshore wind farm, and

the encoding type is real. The second part of the cable connection is encoded as an integer using the principle of the minimum spanning tree in the following approximate way. Define sets A and B to represent the node groups within the spanning tree. Designate point A as the initial node and point B as the terminal node, where the cable connection encoding corresponds to the edge's weight. The integer L identifies the edge with the  $L^{\text{th}}$  highest weight. Once a connection is established, the endpoint of the connection is added to set A and removed from set B. The second part of the  $i^{\text{th}}$  dimension takes values ranging from 1 to  $(M+N-i) \times i$  where the connection model is encoded with an index. Let there be a total of T models of cables, sorted by the size of cross-sectional area, then the range of values of the dimensions in the third part is 1~T.

### *3.2.2. Normalized Difference Degree Representation Method*

Given that traditional methods relying on Euclidean geometric distances to represent disparities are ineffective in addressing the highly intricate scenarios involving variables, a normalized difference degree representation method is introduced.

The niche strategy for addressing continuous multimodal optimization problems typically segregates the population into several subpopulations predicated on the Euclidean distance between individuals in the search space. However, for discrete domain optimization models encapsulated by coding schemes, this partitioning approach fails to accurately capture the distinctions among individuals and is prone to overlooking dimensions with less pronounced differences in values. Drawing from the conventional species evolution niche strategy, this paper introduces the concept of a normalized difference degree and proposes a niche grouping strategy predicated on this special difference degree. This strategy quantifies the degree of difference between individuals by computing the normalized value of the difference relative to the entire population, rather than relying on the spatial Euclidean geometric distance. For multimodal optimization problems with multiple dimensions, the normalized difference degree between individuals under each dimension is calculated separately, and the sum

is expressed as the overall difference degree between individuals by the ratio of the modal quantity. The difference degree formula is as follows:

$$D_{(p_i,p_j)} = \frac{\sum_{k=1}^n \frac{d_{ij}^k - d_{min}^k}{d_{max}^k - d_{min}^k}}{n} \quad (11)$$

where  $n$  denotes the number of dimensions,  $d_{ij}^k$  denotes the difference between individuals  $i$  and  $j$  in the  $k$ th dimension,  $d_{max}^k$ 、 $d_{min}^k$  denotes the maximum and minimum difference between particles in the  $k$ th dimension, respectively, and  $D_{(p_i,p_j)}$  calculates the ratio of the sum of the difference rates of all dimension comparison parameters to the number of dimensions, which is denoted as the overall difference degree. After normalization, Eq. (11) yields an inter-particle variability between 0-1.

For the tackled model, the variation in substation location is quantified by the planar distance between the positions of the two solutions' substations. The discrepancies in topology connections and cable selection are quantified by the differences in the connection status at corresponding positions within the topology connection matrix. The specific procedure is delineated as follows: upon acquiring the connectivity matrix of the offshore wind farm's collection system topology, a Boolean value is employed to signify the presence or absence of a direct cable link between any two wind turbines. In comparing two distinct tree topology connectivity matrices, a bitwise comparison is conducted. Discrepancies in the values at corresponding positions suggest that the connectivity status of the respective wind turbines differs, and 1 is added when calculating the difference degree. The difference degrees at all positions are summed to obtain the particle topology connection difference, and the topology connection difference degree can be obtained according to Eq. (11).

### 3.2.3. Grouping and Population Balance Strategy Based on NBMA Algorithm

Unlike the single-modal optimization algorithm, the multimodal algorithm needs to take into account the distance between particles and their mass when solving. To concurrently assess an individual's level of disparity and fitness, this study introduces a metric that represents the attraction to particles. This metric is calculated as the product of the normalized disparity degree and the fitness value, as follows:

$$A_{(p_i,p_j)} = D_{(p_i,p_j)} \cdot F_j \quad (12)$$

where  $F_j$  denotes the fitness value of individual  $j$ .  $A_{(p_i,p_j)}$  calculates the attractiveness value of individual  $j$  to individual  $i$ .

By doing so, the individual with the smallest attraction value is the most attractive individual for that particle, i.e., Nearest Better Most Attractive (NBMA) individual. This method allows the particle to select the relatively nearest optimal individual instead of the absolute nearest and global optimal individual as the evolutionary direction, taking into account the small habitat convergence and global optimization search.

The efficacy of multimodal algorithms is significantly influenced by the quality of groupings. A large subpopulation may overlook multimodal characteristics, whereas a small one might squander computational resources. Consequently, it is imperative to regulate the grouping process. In this study, the regulation of subpopulation numbers is achieved by employing strategies that involve merging populations and limiting the maximum size of populations. The population size  $k$  is determined by the attraction of the subpopulation optimal particle to the remaining particles. The point with the largest slope of the attraction is taken as the boundary of the subpopulation. In addition, this algorithm limits the subpopulation size by the ratio of the maximum number of individuals in the subpopulation to the total number of individuals, which is defined as  $a$  and calculated by

$$a = \frac{Size_{subpop}}{Size_{totalpop}} \quad (13)$$

where  $Size_{subpop}$  is the maximum number of individuals in the subpopulation and  $Size_{totalpop}$  is the total number of individuals. When the number of individuals in the subpopulation is not greater than  $a$ , the self-population generation step is continued, and vice versa, the current subpopulation generation cycle is exited.

After forming the seed  $S_i$  of a population, when the seed  $S_j$  of another population is in close proximity to the previous population  $S_i$ , it may lead to an overlapping effect on the seeds  $S_{j1\_seed}, S_{j2\_seed}, \dots, S_{jN\_seed}$  of the other population, thereby creating complications. The population merging mechanism is depicted in Figure 6.

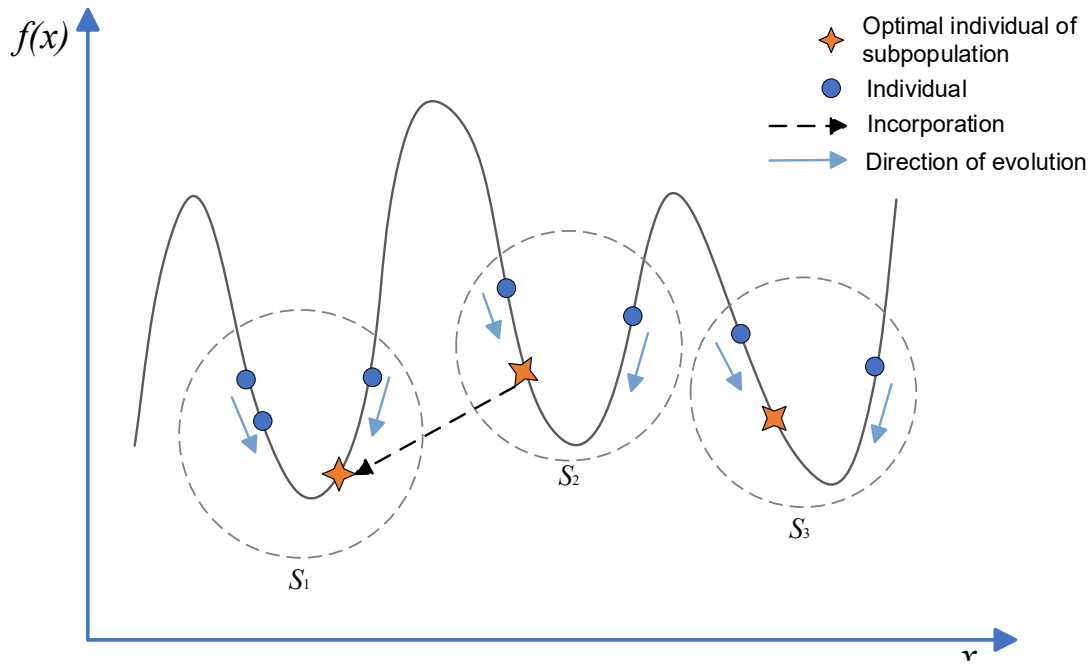


**Figure 6 Population Merging Mechanism**

The objective of the merging strategy is to reassess and reorganize populations deemed suboptimal. This approach takes into account not only the fitness of individuals within their respective populations but also their relative fitness when compared to adjacent populations. By minimizing the fitness cost within the population and achieving a more refined solution in the layout system, the merging strategy is pivotal for ultimately enhancing cost efficiency. In Figure 6,  $S_1, S_2, S_3$  are examples of populations formed based on the fitness function, with the circular areas representing the search domains of each population. The rule for population merging is that  $S_1$  is considered to be dominated by  $S_2$  only if every individual within  $S_1$  is inferior to the individual with the lowest fitness value of  $S_2$ , according to the objective function within the population. Despite one individual in the population  $S_1$  having the lowest fitness cost, population  $S_3$  will not merge with population  $S_1$  because the distance between them is sufficiently large to allow seed  $S_{j3\_seed}$  to still influence seed  $S_{j1\_seed}$ . Based on the above preparations, the NBMA algorithm grouping strategy is summarized in Table 3.

**Table 3 NBMA algorithm grouping strategy**

---

Input: Original population and fitness values

Output: Locally optimal and most attractive individuals for every particle

---

- 1: Calculate the maximum attractive individual for every particle according to formula (12)
  - 2: while the original population is not empty
  - 3:   Sort the fitness of the original population
  - 4:   Take the best individual  $X_{\text{best}}^k$  as one of the seeds
  - 5:   calculate parameter  $k$ , the size of the sub-population by attraction matrix
  - 6:   ensure that  $k < a$
  - 7:   remove the  $k$  particles from the original population that are most attracted by the seed
  - 8: end while
  - 9: for all individuals
  - 10:   find the seed  $X_{\text{best}}^i$  that attracts to it the most
  - 11:   find the particle  $X_i$  that attracts to it the most
  - 12:   Use  $X_{\text{best}}^i$  as the locally optimal individual for this particle
  - 21:   Use  $X_i$  as the most attractive individual for this particle
  - 22: end for
- 

#### *3.2.4. Two-Stage Improved PSO Algorithm Based on Prim Initialization*

When employing the PSO algorithm, it is essential to initiate the population, often through a random initialization approach [677,68]. However, the collection system topology optimization model involves high dimensionality and computational complexity, so this random initialization method is inefficient. Therefore, this paper combines the Prim algorithm for population initialization and grouping of turbines. The Prim algorithm can consider the wind turbines as nodes of the graph, the cable connections as edges, and the lengths of the cables as the weights of the edges. By



$$V(t + 1) = \left(1 - \frac{t}{T}\right) \cdot V(t) + c_1 \cdot rand \cdot (pbest_i(t) - X(t)) + c_2 \cdot rand \cdot (Guide(t) - X(t)) \quad (14)$$

$$X(t + 1) = X(t) + V(t + 1) \quad (15)$$

where  $V(t + 1)$  is the velocity of the  $(t + 1)$ th generation of the particle in the second stage,  $t$  is the index number of generations, and  $T$  is the total number of iterations.  $X(t + 1)$  is the position of the particle in the  $(t + 1)$ th generation,  $pbest_i$  is the best position of the particle over the generations,  $Guide$  is the most attractive particle position of the individual in the first stage, and the locally optimal individual in the second stage,  $\omega$  is the inertia factor, and  $c_1, c_2$  are the learning factors.

### 3.3. Model Solving Process

The solution procedure is depicted in Figure 8 and primarily consists of the initialization phase, subpopulation generation, and evolution based on the PSO algorithm. The initialization phase involves configuring wind farm data and algorithmic parameters, randomly assigning particle velocities, and initializing the tree topology using Prim's algorithm.

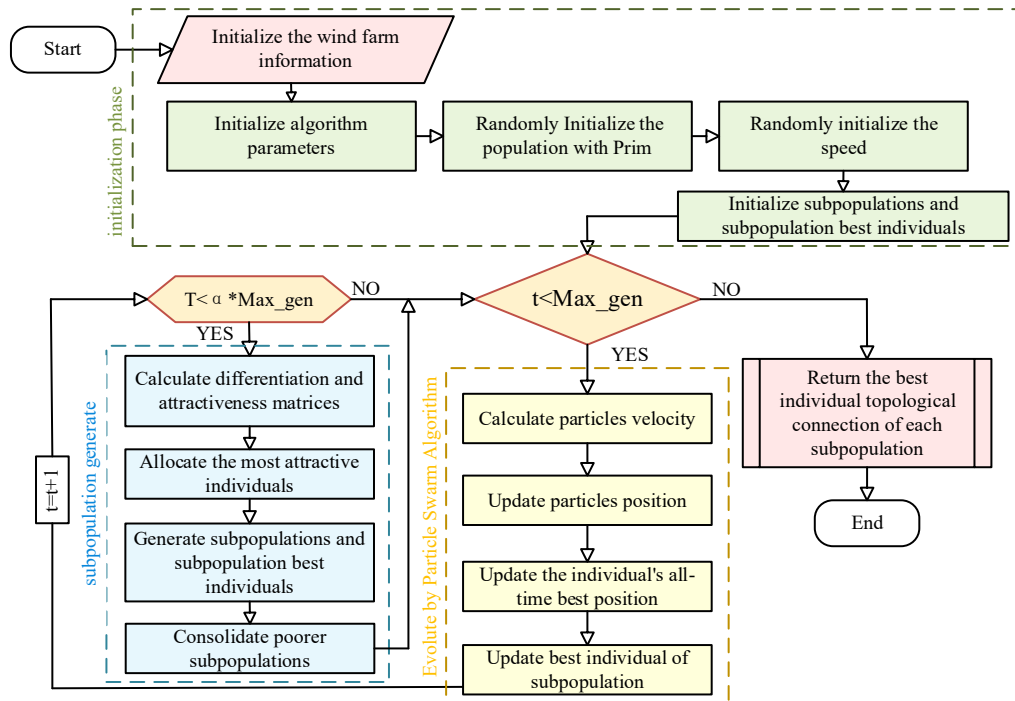


Figure 8 Model Solving Flowchart

#### 4. Algorithm Test on CEC Multi-Peak Function

To better verify the superiority of the NBMA-PSO algorithm, standard CEC multi-peak test functions are used for testing, and the performance of NBMA-PSO is compared with that of the advanced Niche-PSO [57] and Species-PSO [58] algorithms.

The three multi-peak functions selected in this section test the algorithm's capabilities in global search, local optimization accuracy, and dynamic adaptation, respectively. The multimodal characteristics of each function and the corresponding algorithm performance requirements are shown in Table 4.

**Table 4 Test functions and their respective characteristics**

Function	Multimodal characterization	Requirements for algorithm performance
Fractured Terrain	Stochastic fragmented multi-peak distribution	Gradient-free global exploration, out-of-local-optimality capabilities
Panning Griewank	Periodic translational multi-peak system	Dynamic Optimal Tracking, Historical Information Utilization
Composite Schwefel	Heterogeneous partitioned multimodal distribution	Mutation boundary identification, region adaptive optimization

The above test functions cover different types of multimodal problems ranging from simple periodic multi-peaks to complex nested multi-peak structures, which can effectively and comprehensively evaluate the performance of the algorithms in different optimization scenarios. The NBMA-PSO, Niche-PSO, and Species-PSO algorithms were each run independently 10 times, and the parameter settings for each algorithm are shown in Table 5. Figure 9 and Table 6 show the test results, respectively, and each data point is the average of multiple runs.

**Table 5 Algorithmic parameter**

NBMA-PSO	Niche-PSO	Species-PSO
$w = 0.729$	$w = 0.729$	$w = 0.729$
$c_1 = 1.49$	$c_1 = 1.49$	$c_1 = 1.49$

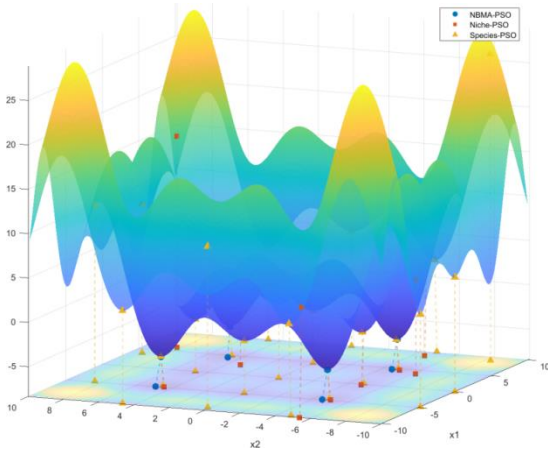
$c_2 = 1.49$	$c_2 = 1.49$	$c_2 = 1.49$
$\alpha = 0.2$	$radius = 0.1 \times norm(ub - lb)$	$radius = 0.1 \times norm(ub - lb)$

By analyzing the operation results of the three algorithms in Table 6 on the above test functions with different multimodal characteristics, it can be found that NBMA-PSO demonstrates a more significant advantage in terms of both global search capability and local development accuracy. In terms of global optimization ability, NBMA-PSO finds no more optimal values than the other two algorithms on the three tested functions, and can effectively find near-global optimal solutions. In the Fractured Terrain function, the mean value of NBMA-PSO is -2.634, which indicates that it can effectively explore globally and avoid falling into local optimal solutions in the randomly fragmented multi-peak distribution. In the Composite Schwefel function, the mean value of NBMA-PSO is 0.625, which is much lower than the 3.241 achieved by Species-PSO. This further indicates that NBMA-PSO effectively avoids local optima in heterogeneous, partitioned multi-peak distributions and maintains stable global search performance. In terms of local exploitation accuracy, NBMA-PSO also shows superior performance. In the Panning Griewank function, the mean value of NBMA-PSO is 0.037, and the RMS is 0.066, which indicates that it can effectively track the dynamic optimal solution in the periodic translational multi-peak system and maintain a high local exploitation accuracy. In contrast, Niche-PSO and Species-PSO exhibit large fluctuations in local development accuracy in complex problems.

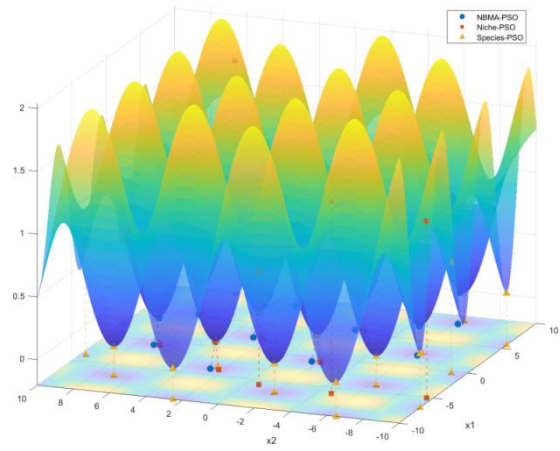
**Table 6 CEC test function result table**

Function	Algorithm	Best	Worst	Mean	RMS	Count	Runtime
Fractured Terrain	NBMA-PSO	<b>-4.984</b>	<b>2.068</b>	<b>-2.634</b>	4.241	6	<b>0.294</b>
	Niche-PSO	-4.984	13.533	0.772	7.813	7	0.925
	Species-PSO	-4.984	10.119	1.194	<b>4.205</b>	22	1.411
Panning Griewank	NBMA-PSO	<b>0.000</b>	<b>0.208</b>	<b>0.037</b>	<b>0.066</b>	12	<b>0.329</b>
	Niche-PSO	0.000	1.058	0.334	0.524	7	1.008
	Species-PSO	0.000	1.312	0.176	0.370	20	1.561
	NBMA-PSO	<b>0.093</b>	<b>0.914</b>	<b>0.625</b>	<b>0.729</b>	4	<b>0.341</b>

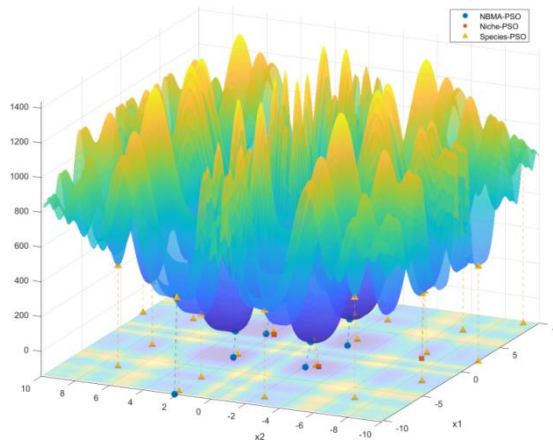
Composite	Niche-PSO	0.093	8.230	3.388	4.584	4	1.018
Schwefel	Species-PSO	0.093	8.591	3.241	4.029	21	1.470



(a) Fractured Terrain



(b) Panning Griewank



(c) Composite Schwefel

Figure 9 CEC test function result graph

## 5. Case Study

This paper selects an offshore wind farm in Zhuhai (Guishan, China) for a validation case. The collection system of this wind farm connects one substation and 27 wind turbines. All wind turbines are of the same model, and the parameters of the proposed wind turbines are summarized in Table 7.

Table 7 Wind Turbine Parameters

Turbine Power	Blade Radius	Hub Height	Cut-in Wind Speed	Rated Wind Speed	Cut-out Wind Speed
10MW	89.15m	119m	4m/s	11.3m/s	25m/s

Converting the orientation of the wind turbines to the coordinate plane, their arrangement is shown in Figure 10.

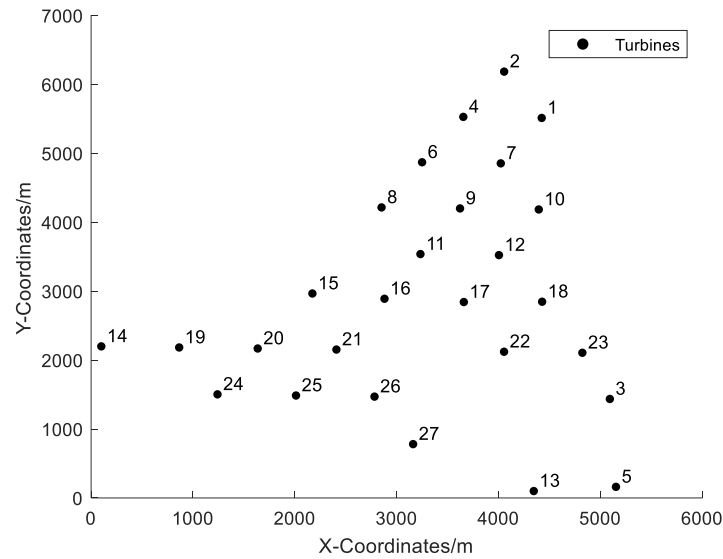


**Figure 10** Layout of Wind Turbines in Guishan Wind Farm

The two-parameter Weibull distribution of wind speed is employed to estimate the power generation of the wind turbines. The wind speed distributions for different wind directions were calculated from the Weibull distribution. The wind rose plot considering the Weibull distribution is shown in Figure 11.

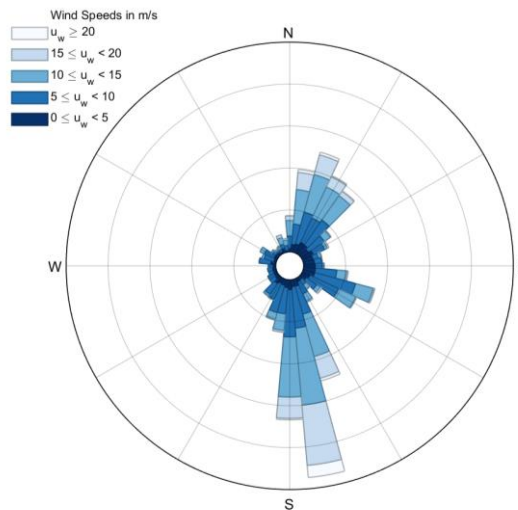


**Figure 11** Wind Rose Diagram

For cable selection, the model parameters are determined based on the rated voltage of the collection system, 35 kV, as summarized in Table 8.

**Table 8 Cable Parameters**

Cable cross section / $mm^2$	Resistance / ( $\Omega \cdot km^{-1}$ )	Maximum Current / $A$	Unit Price / (RMB · $m^{-1}$ )
50	0.387	175	981
95	0.913	255	1221
150	0.124	335	1491
240	0.0761	430	1772
400	0.0481	550	2302
500	0.0449	630	2811

### 5.1. Optimal results under different parameters

Multimodal algorithms can find multiple feasible solutions simultaneously, not just the global optimal solution. The number of modes formed is related to the maximum subpopulation size parameter ( $a$ ), which ranges from 0 to 1.

Figure 12 shows the number of subpopulations, i.e., the modal number, obtained by the algorithm for different values. When  $a = 1$ , the number of subpopulations is approximately 1; when  $a = 0.5$ , it is approximately 3; when  $a = 0.2$ , it is approximately 6; and when  $a = 0.1$ , it is approximately 11. Clearly, as  $a$  approaches 1, the NBMA algorithm gradually loses its multimodal characteristics, and the largest subpopulation almost encompasses the entire search space, leading to unimodal. Conversely, smaller  $a$  can lead the algorithm to generate an excessive number of subpopulations, where a few or even a single particle might be erroneously identified as a distinct mode. On one hand, this results in suboptimal solution quality, failing to satisfy the criteria for economic efficiency and high reliability. On the other hand, the convergence of particles in less favorable regions leads to a significant waste of sample data. Consequently, to preserve the algorithm's multimodal capabilities and ensure solution quality, the selection of  $a$  must be approached with caution and precision.

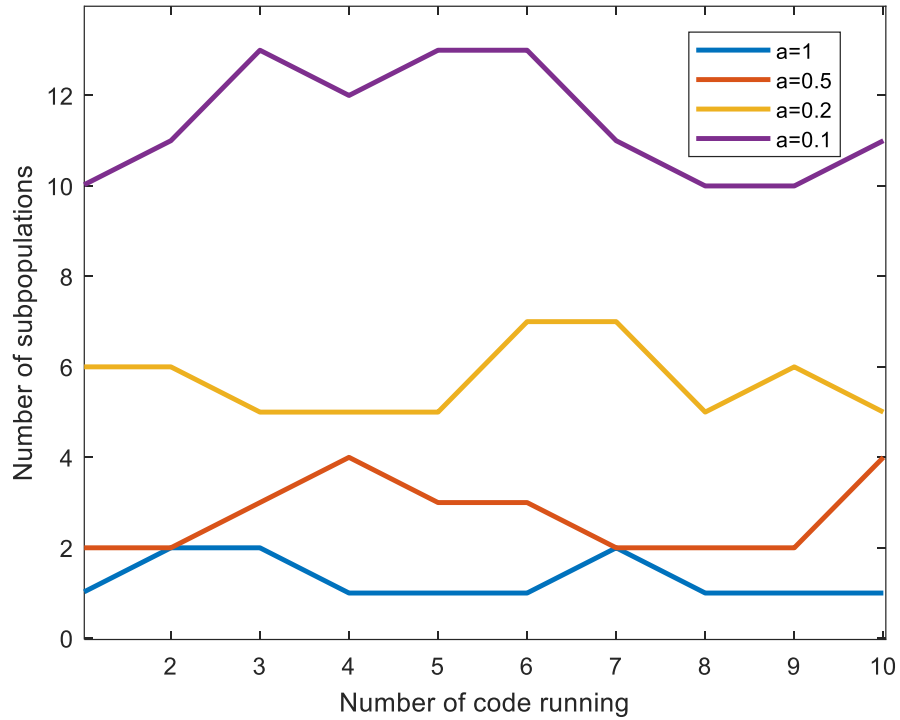


**Figure 12** Number of Subpopulations for Different Parameters

When  $a = 0.5$ , the topological structures of the three different modalities are shown in Figure 13. From Figure 13, the commonalities of the different modalities are as follows: (1) Topological connections: Due to the low density of wind turbines at the edges of the wind farm and the only possible connection between two edge turbines, The topological connections at the edges of the three modalities are the same; (2) Cable selection: Cables with a cross-sectional area of  $50\text{mm}^2$  are mainly used. This is attributed to the fact that smaller cross-sectional cables are more cost-effective for conducting relatively low currents, hence they are predominantly utilized at the periphery of the wind farm, where power generation is less substantial. (3) Substation location: The substation is located at the center of the wind farm. Since long-distance transmission increases energy loss costs and cable investment costs, the substation is located at the center of the wind farm in each modality to shorten the transmission distance and improve system stability.

The differences between modalities are as follows: (1) Regarding the topological connection, there are certain differences in the topological connections corresponding to the three different modalities, especially in areas with a high density of wind turbines; (2) Regarding the selection of cables, the variation in topological connections leads to differences in the current-carrying capacity of cables at the same location across various

modalities. Consequently, the determination of the cable cross-sectional area must be based on the magnitude of the current-carrying capacity to select the most appropriate solution. This results in substantial differences in cable selection among the different modalities.

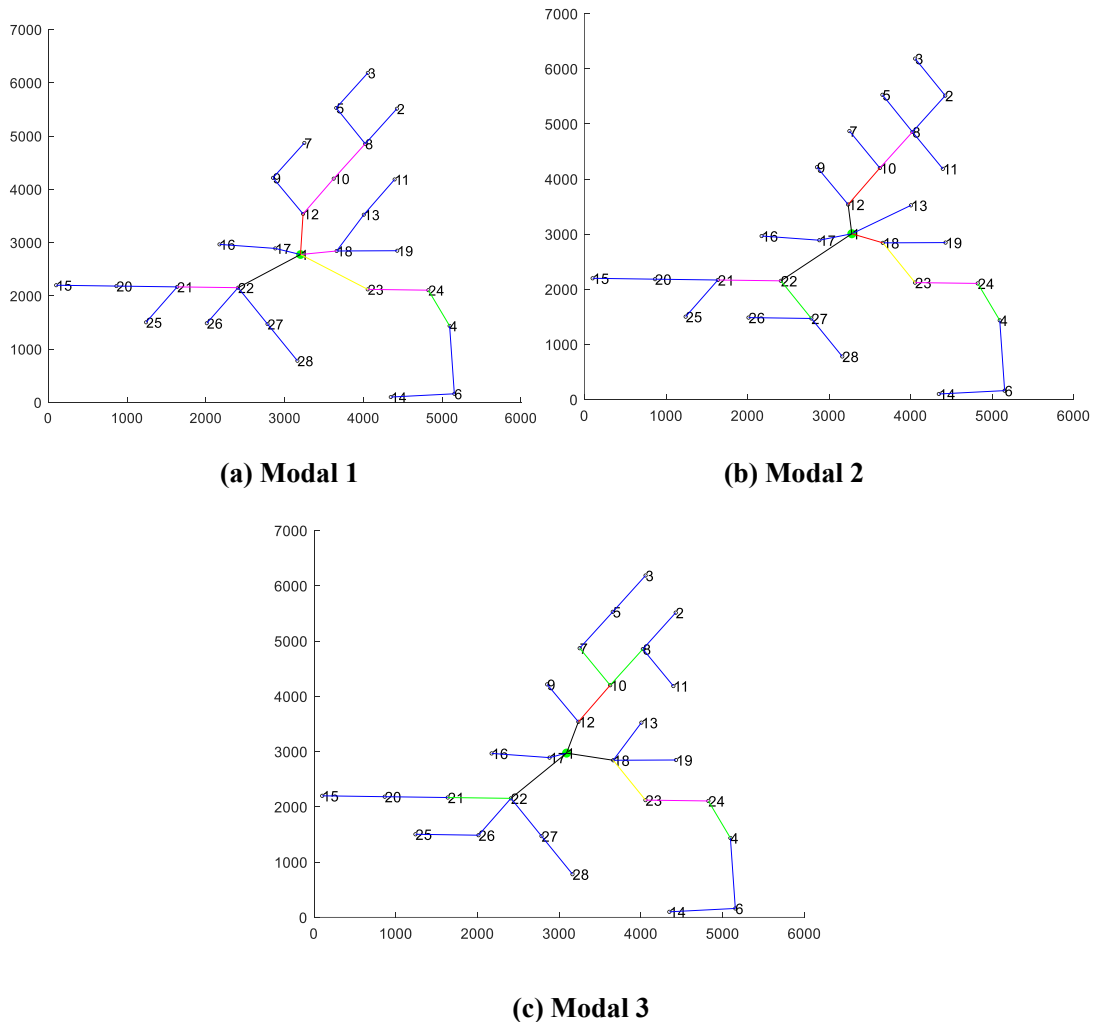


**Figure 13** Schematic diagram of the topology of each Modal (Point 1 is the substation location, Points 2-28 are the wind turbine locations, solid lines represent cable connections; different cross-section areas of the cables are distinguished by colored lines, with blue, green, pink, yellow, red, and black respectively representing 35kV cables with cross-sectional areas of 50mm<sup>2</sup>, 95mm<sup>2</sup>, 150mm<sup>2</sup>, 240mm<sup>2</sup>, 400mm<sup>2</sup>, and 500mm<sup>2</sup>.)

The fitness curve plays a crucial role in the algorithm for optimizing comparisons between different modalities, providing real-time feedback on its performance, convergence characteristics, and efficiency. The fitness curves for the three modalities are depicted in Figure 14, showing the iteration process of different modalities by comparing the changes in fitness during the iteration process. Modal 2 demands the highest number of iterations to identify the cable configuration with the lowest cost,

with modal 3 requiring approximately 250 iterations, whereas modal 1 requires the fewest, around 230 iterations. It is worth noting that all modalities exhibit a step pattern, with no abrupt changes in the convergence curve. The fitness value for Modal 1 is 120.61 million RMB, while the minimum cost for Modal 2 is 122.02 million RMB, and Modal 3 shows 123.13 million RMB. The findings presented above demonstrate that the proposed NBMA-PSO algorithm is capable of discovering multiple high-quality solutions, thereby facilitating enhanced decision-making processes.

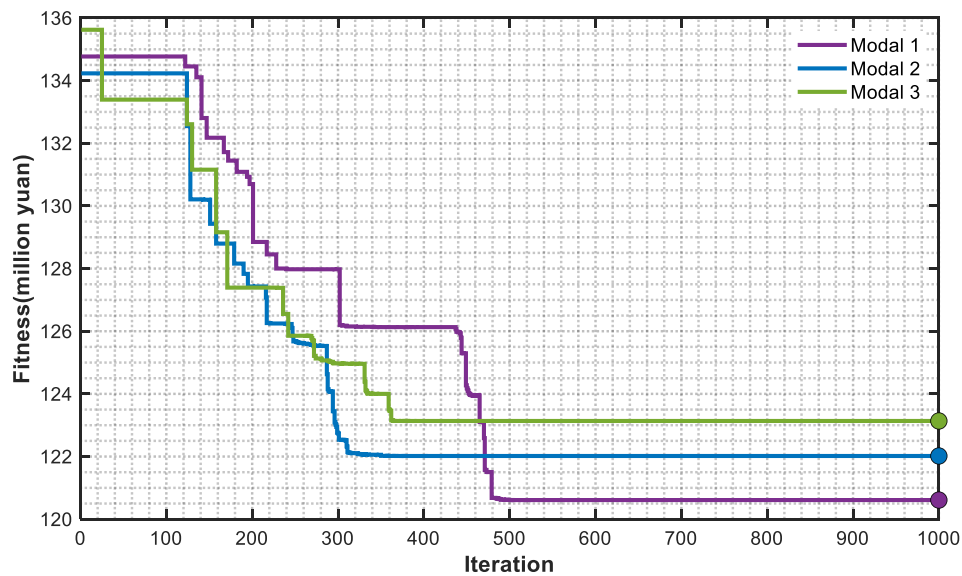


**Figure 14** Fitness curves of each Modal

## 5.2. Comparison of modals under wind direction and speed fluctuations

Owing to the inherent unpredictability of wind, the fitness function value of a solution derived from anticipated wind conditions may be subject to alteration in the event of shifts in wind direction or reductions in wind speed. In this investigation, the three modalities depicted in Figure 13 are subjected to a thorough analysis under the influence of variable wind conditions.

Considering the wind direction shifting from  $-40^{\circ}$  to  $+30^{\circ}$ , the values of the fitness function corresponding to the three modalities are calculated and shown in Figure 15. Although the total cost corresponds to all three modal changes with the shift of wind direction, the magnitude of their changes varies. When the wind is deflected clockwise, the total cost of mode 1 shows a decreasing and then increasing trend. When the wind direction is deflected clockwise by  $10^{\circ}$ , the total cost is about RMB 115.72 million, a

decrease of about 4.1%. As the wind continues to deflect clockwise, the total cost starts to rise. When the wind is deflected 25° clockwise, the total cost shows a slight decrease and then continues to rise. When the wind direction is deflected by 30°, the total cost is about 130.38 million RMB, an increase of about 8.1%. The changing trends of mode 2 and mode 3 when the wind is deflected in the clockwise slice are basically consistent with this. When the wind is deflected counterclockwise, the total cost shows the same trend of decreasing and then increasing, but more gently. The total cost within 40 degrees of the counterclockwise deflection is lower than the no-deflection case. This may be due to the fact that the suppression of wake effects by the turbine layout is no longer effective in this case, resulting in lower current loads and savings in energy loss costs. It is worth noting that Modal 1 has the lowest total cost in any wind direction, showing strong robustness. Although the total cost of Modal 3 is significantly higher than that of Modal 2 when the wind direction is fixed, the total costs of these two modals are very close to each other when the wind direction is deflected. This should be one of the important bases for the final topology selection.

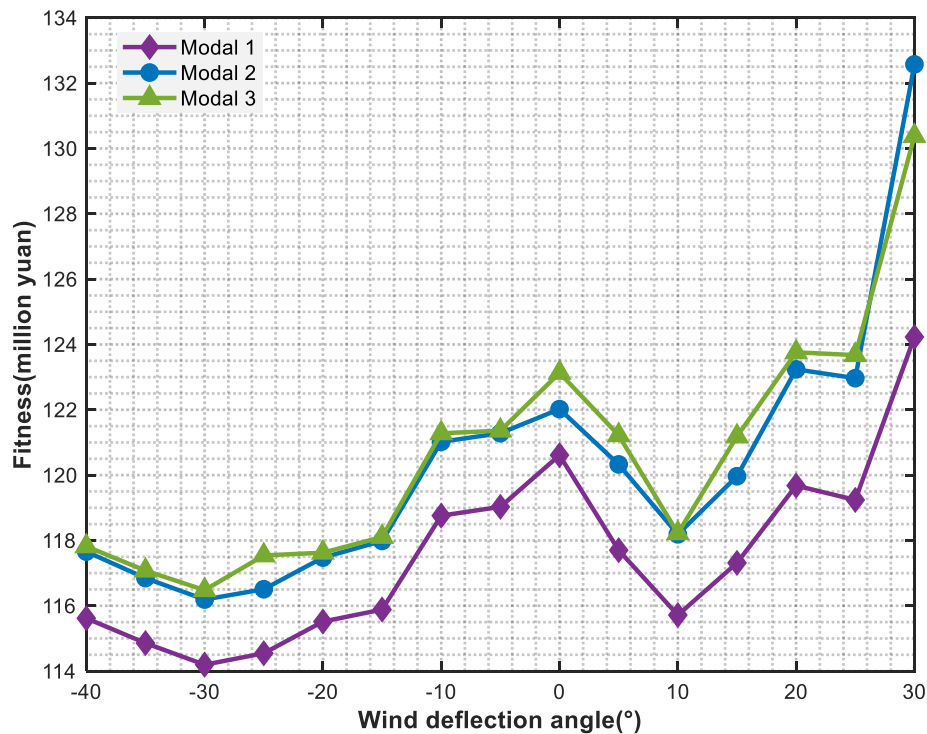


**Figure 15** Changes in fitness function values of the three modal under the shifting wind direction

Similarly, when there is a change in wind speed, the total cost of the collection system for the three modalities is calculated and depicted in Figure 16. An increase in wind speed results in enhanced power generation from the turbines, which in turn leads to a significant rise in the energy loss cost, ultimately contributing to an increase in the total construction cost. As the wind speed increases, the total cost associated with each modal nearly continues to escalate. When the wind speed is below the threshold wind speed, although Modal 1 remains more cost-effective than Modal 2 and 3, the difference in total costs among them is not markedly pronounced. All remain at around 1%. When the wind speed further increases, the total cost of Modal 1 and 2 can still maintain a rapidly increasing trend. When the wind speed increases by 5%, the total cost of modal 1 and 2 increases by approximately 3.1% and 8.3%, respectively, compared to the original wind speed. Modal 3 gradually demonstrated its superiority. When the wind speed increases by about 8%, modal 3 surpassed modal 1 to become the optimal solution, with a total cost of about 128.03 million RMB. When the wind speed increases by 10%, the total cost of modal 3 decreases by about 1.6% and 6.3% compared to modal 1 and 2, respectively, demonstrating its superiority.

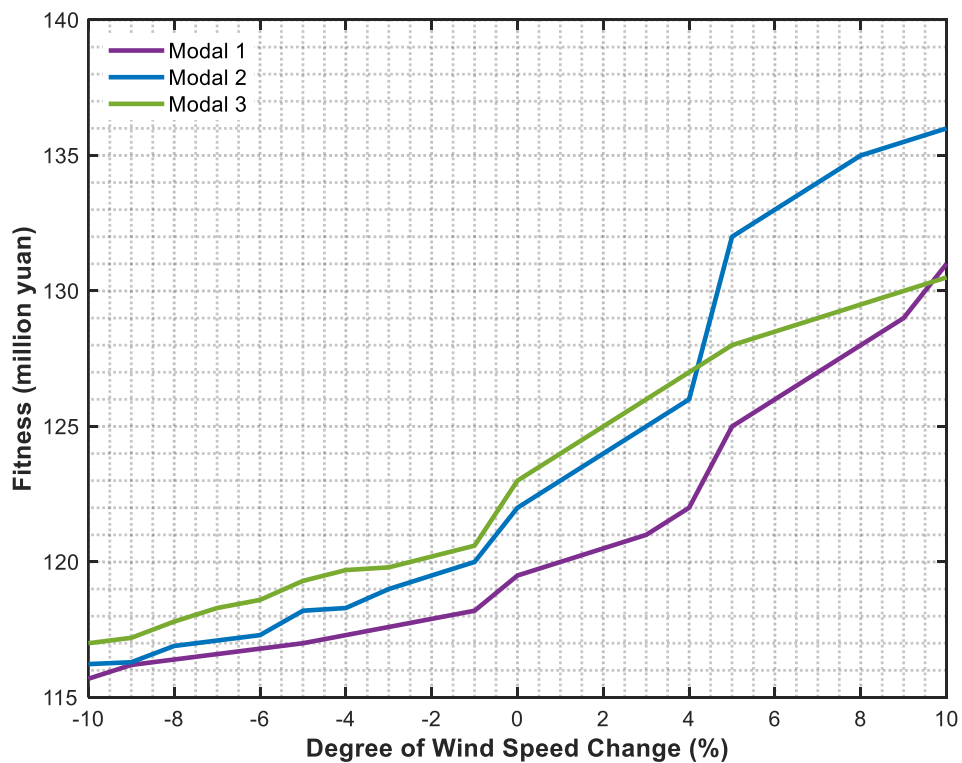


**Figure 16** Changes in fitness function values for three modal when wind speed changes

### 5.3. Comparison of optimization results under different algorithms

PSO algorithm and the Aquila Optimization (AO) algorithm are commonly used, which have shown good performance in solving nonlinear problems such as offshore wind farm collection systems optimization. The NBNC-PSO algorithm combines the PSO algorithm efficiency with the grouping strategy of the NBNC algorithm for obtaining a solution, which has shown good performance in the offshore wind farm collection systems optimization [38]. To compare them, the three algorithms and the proposed NBMA-PSO algorithm are run ten times, and their results with box plots are shown in Figure 17.

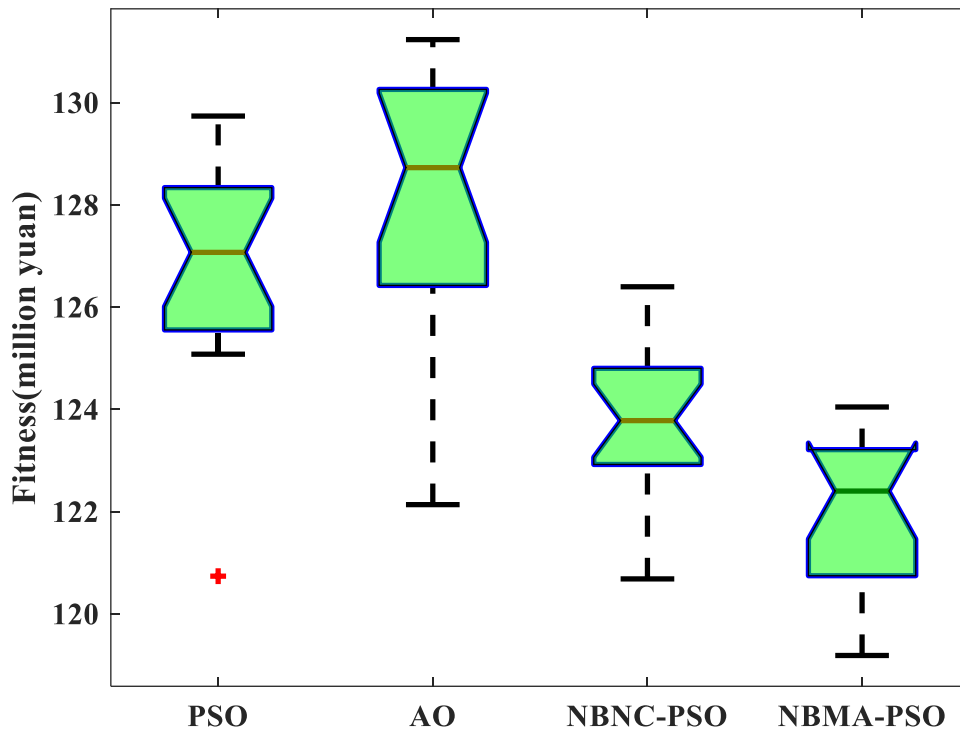


Figure 17 Box Plot of Costs for Different Algorithms

Meanwhile, Table 9 lists the optimal total cost, average total cost, and modal number obtained by the above four algorithms. The traditional PSO algorithm and AO algorithm run stably, but they usually fall into local optimal solutions, thus failing to find the global optimal position. As multimodal algorithms, NBNC-PSO and NBMA-PSO algorithms are far superior to the first two algorithms in global search capability, not only being able to simultaneously obtain multiple modal solutions but also being

more likely to find the global optimal position. It is worth noting that the NBMA-PSO algorithm has the best performance. Compared to PSO, AO, and NBNC-PSO, the optimal total cost obtained by the NBMA-PSO algorithm is reduced by 4.1%, 1.9%, and 0.5%, respectively, and the average total cost is reduced by 4.3%, 4.2%, and 0.2%, respectively.

**Table 9 Performance Comparison Among Algorithms**

Algorithm	PSO	AO	NBNC-PSO	NBMA-PSO
Optimal Total Cost (million RMB)	125.1	122.3	120.7	120.0
Average Total Cost (million RMB)	128.2	128.0	122.9	122.6
Modal Number (-)	Single	Single	Multiple	Multiple

#### **5.4. Limitations and engineering applications**

In this subsection, the limitations of this study are first presented. Then it explains how decision makers can apply the multimodal solutions derived from the algorithm in real engineering.

##### *5.4.1. Limitations of the study*

Although the proposed method has significant advantages for the topology design of offshore wind farm collection systems, there are still some limitations that need to be considered in future research. The following points outline these shortcomings.

- Optimizing the collection system of offshore wind farms relies on mathematical models. However, the dynamic marine environment could lead to substantial discrepancies between these models and actual scenarios. While multimodal algorithms provide multiple optimal solutions, they may not always align with practical requirements. Future research could benefit from incorporating robust designs to address this issue.

- The Weibull wind speed distribution and the Jensen wake model do not describe the wind conditions with complete accuracy. In this paper, these two models with acceptable accuracy are chosen for computational efficiency. In order to model wind farms more accurately, a proxy model approximation or simulation is required. This needs to be emphasized in subsequent studies. This study does not delve into the pertinent concerns regarding the protection of the marine ecological environment and maritime safety. The implications for the feasibility of modal selection necessitate further analysis by designers. Future research should address these issues with multi-objective designs.
- Given the limited adoption of discrete multimodal algorithms, this study only compared the proposed NBMA-PSO with the NBNC-PSO algorithm in the wind farm arithmetic study. A comparison with additional sophisticated multimodal algorithms would further accentuate the comparative advantages and limitations of the proposed algorithm.

#### *5.4.2. Engineering applications*

In real engineering applications, decision makers need to synthesize a variety of factors, such as policy, construction, budget, and wind direction, to choose among multimodal solutions.

Firstly, the decision maker should assess whether any policy changes have resulted in increased constraints. If such changes exist, non-compliant or suboptimal solutions must be eliminated.

Secondly, due to significant uncertainties in wind direction and wind speed, it is necessary to analyze how the costs of solutions obtained by the multimodal algorithm vary under changes in these parameters. If the total cost of the optimal solution for a fixed wind direction increases substantially compared to other suboptimal solutions when the wind direction shifts, this optimal solution should not be selected either.

Finally, it is important to choose a topology based on budget. Decision makers need to choose the desired balance between economy and reliability, as economy goals and reliability goals are usually highly conflicting.

## 6. Conclusion

This study tackles the challenge of topology optimization for offshore wind power collection systems, considering capital cable costs, cable installation, and energy loss. It incorporates the Weibull wind speed model and the Jensen wake model to formulate a more scientifically robust and rational cost model. To address this optimization problem, a novel multimodal algorithm, termed NBMA-PSO, has been introduced, which is capable of providing multiple optimal solutions to meet real-world design specifications. The efficacy of the algorithm is validated through case studies, where it demonstrates superior performance over PSO, AO, and NBNC-PSO in terms of reduced optimization costs. Future research will investigate the integration of wind turbine placement into the optimization model by considering the need for multi-objective robust designs.

## References

- [1] Ji L, Li J, Sun L, Wang S, Guo J, Xie Y, et al. China's onshore wind energy potential in the context of climate change. *Renewable and Sustainable Energy Reviews* 2024;203:114778. <https://doi.org/10.1016/J.RSER.2024.114778>.
- [2] Ren Z, Verma AS, Li Y, Teuwen JJE, Jiang Z. Offshore wind turbine operations and maintenance: A state-of-the-art review. *Renewable and Sustainable Energy Reviews* 2021;144:110886. <https://doi.org/10.1016/J.RSER.2021.110886>.
- [3] Zhang J, Zhang J, Cai L, Ma L. Energy performance of wind power in China: A comparison among inland, coastal and offshore wind farms. *J Clean Prod* 2017;143:836–42.
- [4] Park, C., Shin, S. W., Cha, D. H., Min, S. K., Byun, Y. H., Kim, J. U., & Choi, Y. (2024). Impact of global warming on wind power potential over East Asia. *Renewable and Sustainable Energy Reviews*, 203, 114747.
- [5] Si, G., \*\*a, T., Gebraeel, N., Wang, D., Pan, E., & \*\*, L. (2025). Holistic opportunistic maintenance scheduling and routing for offshore wind farms. *Renewable and Sustainable Energy Reviews*, 207, 114991.

- [6] Sykes, V., Collu, M., & Coraddu, A. (2023). A review and analysis of the uncertainty within cost models for floating offshore wind farms. *Renewable and Sustainable Energy Reviews*, 186, 113634.
- [7] Li Lingfei, Sun Yue, Huang Ying, et al. Reliability evaluation of offshore wind farms and VSC-HVDC system considering the impact of severe weather . *Southern Power System Technology*, 2020, 14(12): 32-42.
- [8] Zhang Kaihua, Zhang Zhiwei, Jiang Chuanwen, et al. Reliability assessment of offshore wind farm collection system based on the minimum path method. *Low Voltage Apparatus*, 2018, 000(009): 43-47, 59.
- [9] Quinonez-Varela G, Ault GW, Anaya-Lara O, et al. Electrical collector system options for large offshore wind farms . *IET Renewable Power Generation*, 2007(2): 1.
- [10] Wei S, Zhang L, Xu Y, et al. Hierarchical Optimization for the Double-Sided Ring Structure of the Collector system Planning of Large Offshore Wind Farms . *IEEE Transactions on Sustainable Energy*, 2017, 8(3): 1029-1039.
- [11] Wang Jing, Yang Ping, Zhao Zhuoli, et al. Reliability evaluation of the collector system for offshore wind farms based on chain topology . *Renewable Energy*, 2014, 32(10): 1463-1467.
- [12] Wei Shurong, Fan Xiao, Huang Surong, et al. Availability calculation method for the ring structure of the collector system for offshore wind farms . *Journal of Hohai University (Natural Science Edition)*, 2016, 44(01): 89-94.
- [13] Chen Xianhui, Wang Bing, Deng Hongfeng, et al. Analysis of switch configuration for the ring topology structure of the collector system for offshore wind farms . *Renewable Energy*, 2019, 37(02): 205-211.
- [14] Heyman, Olof H., Weimers, Lars, Bohl, Mie-Lotte, et al. Secure, efficient and clean energy systems across borders. *Pro-ceedings of the 21st World Energy Congress (WEC) 2010, Montreal, Quebec, Canada, Sep 12-16, 2010, WEC-2010-237*, 16 pages.
- [15] Gil M D P, J.L. Domínguez-García, F. Díaz-González, et al. Feasibility analysis of offshore wind power plants with DC collection grid . *Pergamon*, 2015.

- [16] Van Eeckhout B, Van Hertem D, Reza M, Srivastava K, Belmans R. Economic comparison of VSC HVDC and HVAC as transmission system for a 300MW offshore wind farm. *Eur T Electr Power*. 2009
- [17] Banzo M, Ramos A. Stochastic optimization model for electric power system planning of offshore wind farms. *IEEE Trans Power Syst*.
- [18] C. Karlsson. Managing harmonics and resonances in HVDC connected 66 kV offshore windfarms. 19th International Conference on AC and DC Power Transmission (ACDC 2023), Glasgow, UK, 2023, pp. 22-29
- [19] Liu Weidong, Xu Han, Feng Jiaqi, et al. Research on the Techno-Economic Feasibility of 66 kV Offshore Wind Power Flexible DC Transmission Scheme. *Proceedings of the 2020 China Communications Society Energy Internet Academic Conference, 2020: 5*.
- [20] ORE Catapult Development Services Limited. 66kV Collector Interface for HVDC. UK Research and Innovation. 131211.
- [21] GIDDANI O A, ADAM G P, LO K L, et al. Grid integration of offshore wind farms using multi-terminal DC transmission systems (MTDC) //5th IET International Conference on Power Electronics, Machines and Drives (PEMD 2010). Brighton, UK: Institution of Engineering and Technology, 2010.
- [22] Liu Weidong, Li Qinan, Wang Xuan, et al. The current status and prospect of large-scale offshore wind power flexible DC transmission technology . *Electric Power*, 2020, 53(7): 55-71.
- [23] Chen Y, Grijalva S, Graber L. Techno-Economical Assessment of MVAC and MVDC Collector systems for Offshore Wind Farms //2023 IEEE Texas Power and Energy Conference (TPEC).0[2024-07-22].
- [24] Timmers V, Agustí Egea-Lvarez, Gkountaras A, et al. All-DC offshore wind farms: When are they more cost-effective than AC designs? . *IET renewable power generation*, 2023(10): 17.
- [25] BAHIRAT H J, MOŘK B A. Operation of DC series-parallel connected offshore wind farm . *IEEE Transactions on Sustainable Energy*, 2019, 10(2): 596-603.

- [26] CHUANGPISHIT S, TABESH A, MOŘADI-SHAHRABAK Z, et al. Topology design for collector systems of offshore wind farms with pure DC power systems . IEEE Transactions on Industrial Electronics, 2014, 61(1): 320-328.
- [27] DAHMĀNI O, BOURGUET S, GUÉRIN P, et al. Optimization of the internal grid of an offshore wind farm using genetic algorithm //IEEE Grenoble PowerTech, June 16-20, 2013, Grenoble, France: 6p.
- [28] Li Dongdong, Li Pengda. Research on the topology structure design of the collection system for offshore wind farms considering restricted areas . Shanghai Vision, 2016, (02): 105-108.
- [29] Huang Wei, Yan Binyu, Tan Maoqiang, et al. Topology design of the collection system for offshore wind farms considering the impact of obstacle areas . Modern Electric Power, 2018, 35(01): 6-13.
- [30] Shen X, Li S, Li H. Large-scale Offshore Wind Farm Electrical Collector system Planning: A Mixed-Integer Linear Programming Approach. 2021.
- [31] R. Chen, Z. Zhang, J. Hu, L. Zhao, C. Li, and X. Zhang, "Grouping-Based Optimal Design of Collector system Topology for a Large-Scale Offshore Wind Farm by Improved Simulated Annealing," in Protection and Control of Modern Power Systems, vol. 9, no. 1, pp. 94-111, January 2024
- [32] Zuo T, Zhang Y, Xiong L, et al. Complete joint-optimization for offshore wind farm planning[J]. International Journal of Electrical Power & Energy Systems, 2024, 157: 109832.
- [33] X. Shen, Q. Wu, H. Zhang, and L. Wang, "Optimal Planning for Electrical Collector system of Offshore Wind Farm With Double-Sided Ring Topology," in IEEE Transactions on Sustainable Energy, vol. 14, no. 3, pp. 1624-1633, July 2023
- [34] Chen Y, Dong Z, Meng K, et al. A novel technique for the optimal design of offshore wind farm electrical layout . Journal of Modern Power Systems & Clean Energy, 2013, 1(3): 258-263.
- [35] Li Pengda, Li Dongdong. Research on the topology structure optimization of the collection system for offshore wind farms . Power System Protection and Control, 2016, 44(18): 102-107.

- [36] Gonzalez-Longatt Francisco M. Optimal Offshore Wind Farms' Collector Design Based on the Multiple Travelling Salesman Problem and Genetic Algorithm. Proceedings of the 2013 IEEE Grenoble Conference, 2013, 16-20 June.
- [37] Zhao Donglai, Niu Dongxiao, Yang Shangdong, et al. Optimization model for the collection topology structure of offshore wind farms based on improved genetic algorithms . Journal of Central South University (Science and Technology), 2019, 50(04): 998-1004.
- [38] Song D, Yan J, Gao Y, et al. Optimization of floating wind farm power collection system using a novel two-layer hybrid method[J]. Applied Energy, 2023, 348: 121546.
- [39] Srikakulapu, R., U, V. Optimized design of collector topology for offshore wind farm based on ant colony optimization with multiple travelling salesman problem. J. Mod. Power Syst. Clean Energy 6, 1181–1192 (2018).
- [40] Zuo T, Zhang Y, Meng K, et al. A two-layer hybrid optimization approach for large-scale offshore wind farm collector system planning[J]. IEEE Transactions on Industrial Informatics, 2021, 17(11): 7433-7444.
- [41] Wu Jin, Mi Zengqiang, Yang Yuxin, et al. Topology optimization of the collection system for large-scale wind farms . North China Electric Power University Journal (Natural Science Edition), 2023, 50(6): 31-39.
- [42] Liu Huaixi, Wu Di, Miao Desheng. Topology optimization design of the collection system for offshore wind farms based on the divide and conquer strategy . Electrical Engineering Technology, 2023, (10): 65-68+72.
- [43] Wang Weiyuan, Qiao Ying, Dou Fei, et al. Topology optimization of the collection system for offshore wind farms based on improved genetic algorithms . Electric Power, 2019, 52(01): 63-68.
- [44] Xiao Z, Jin L, Zheng G. Topology Optimization of Large-scale Offshore Wind Farm Collector Systems Based on Large Language Models [J]. High Voltage Engineering, 2024, 50(07): 2894-2905.
- [45] Zhang, J.; Huang, D.S.; Lok, T.M.; Lyu, M.R. A novel adaptive sequential niche technique for multimodal function optimization. Neurocomputing 2006, 69, 2396–2401.
- [46] Yu, E.; Suganthan, P.N. Ensemble of niching algorithms. Inf. Sci. 2010, 180, 2815–2833.

- [47] Li, X.; Epitropakis, M.G.; Deb, K.; Engelbrecht, A. Seeking multiple solutions: An updated survey on niching methods and their applications. *IEEE Trans. Evol. Comput.* 2016, 21, 518–538
- [48] Li, W., Yao, X., Zhang, T., Wang, R., & Wang, L. (2022). Hierarchy ranking method for multimodal multiobjective optimization with local Pareto fronts. *IEEE Transactions on Evolutionary Computation*, 27(1), 98-110.
- [49] Beasley, D.; Bull, D.R.; Martin, R.R. A sequential niche technique for multimodal function optimization. *Evol. Comput.* 1993, 1, 101–125.
- [50] Brits, R.; Engelbrecht, A.P.; van den Bergh, F. A niching particle swarm optimizer. In *Proceedings of the 4th Asia-Pacific Conference on Simulated Evolution and Learning*, Singapore, 18–22 November 2002; Volume 2, pp. 692–696.
- [51] Liang, J.J.; Qu, B.Y.; Mao, X.; Niu, B.; Wang, D. Differential evolution based on fitness Euclidean-distance ratio for multimodal optimization. *Neurocomputing* 2014, 137, 252–260.
- [52] Yang, Q.; Chen, W.N.; Yu, Z.; Gu, T.; Li, Y.; Zhang, H.; Zhang, J. Adaptive multimodal continuous ant colony optimization. *IEEE Trans. Evol. Comput.* 2016, 21, 191–205.
- [53] Iwase, T.; Takano, R.; Uwano, F.; Sato, H.; Takadama, K. The bat algorithm with dynamic niche radius for multimodal optimization. In *Proceedings of the 2019 3rd International Conference on Intelligent Systems, Metaheuristics & Swarm Intelligence*, Male, Maldives, 23–24 March 2019; pp. 8–13.
- [54] Bo, Q.; Cheng, W.; Khishe, M.; Mohammadi, M.; Mohammed, A.H. Solar photovoltaic model parameter identification using robust niching chimp optimization. *Sol. Energy* 2022, 239, 179–197.
- [55] Li, H.; Zou, P.; Huang, Z.; Zeng, C.; Liu, X. Multimodal optimization using whale optimization algorithm enhanced with local search and niching technique. *Math. Biosci. Eng.* 2020, 17, 1–27.
- [56] Gao, X.Z.; Wang, X.; Zenger, K.; Wang, X. A niching harmony search method for multimodal optimization. In *Proceedings of the 2012 Eighth International Conference on Computational Intelligence and Security*, Guangzhou, China, 17–18 November 2012; pp. 22–27

- [57] T. Crane, B. Ombuki-Berman and A. Engelbrecht, "NichePSO and the Merging Subswarm Problem," 2020 7th International Conference on Soft Computing & Machine Intelligence (ISCMI), Stockholm, Sweden, 2020, pp. 17-22, doi: 10.1109/ISCMI51676.2020.9311551.
- [58] Luo W, Sun J, Bu C, Liang H (2016) Species-based particle swarm optimizer enhanced by memory for dynamic optimization. *Appl Soft Comput* 47:130–140.
- [59] Gu, Q., Niu, Y., Hui, Z., Wang, Q., & Xiong, N. (2025). A hierarchical clustering algorithm for addressing multi-modal multi-objective optimization problems. *Expert Systems with Applications*, 264, 125710.
- [60] Shi, R., Lin, W., Lin, Q., Zhu, Z., & Chen, J. (2019, June). Multimodal multi-objective optimization using a density-based one-by-one update strategy. In *2019 IEEE Congress on Evolutionary Computation (CEC)* (pp. 295-301).
- [61] Song, D., Haq, I. U., Rehman, M. S. U., Dong, M., Noor, J., & Evgeny, S. (2024, May). Multimodal Algorithm for Minimization of Costs in Offshore Wind Farm Collection System. In *2024 IEEE 2nd International Conference on Power Science and Technology (ICPST)* (pp. 1433-1438). IEEE.
- [62] Wędzik A, Siewierski T, Szypowski M. A new method for simultaneous optimizing of wind farm's network layout and cable cross-sections by MILP optimization. *Appl Energy* 2016;182:525–38. <https://doi.org/10.1016/J.APENERGY.2016.08.094>.
- [63] Mohamed AA, Kamel S, Hassan MH, Mosaad MI, Aljohani M. Optimal Power Flow Analysis Based on Hybrid Gradient-Based Optimizer with Moth–Flame Optimization Algorithm Considering Optimal Placement and Sizing of FACTS/Wind Power. *Mathematics* 2022, Vol 10, Page 361 2022;10:361. <https://doi.org/10.3390/MATH10030361>.
- [64] dos Santos FS, do Nascimento KKF, da Silva Jale J, Xavier SFA, Ferreira TAE. Brazilian wind energy generation potential using mixtures of Weibull distributions. *Renewable and Sustainable Energy Reviews* 2024;189:113990. <https://doi.org/10.1016/J.RSER.2023.113990>.

- [65] Dhiman HS, Deb D, Foley AM. Bilateral Gaussian Wake Model Formulation for Wind Farms: A Forecasting based approach. *Renewable and Sustainable Energy Reviews* 2020;127:109873. <https://doi.org/10.1016/J.RSER.2020.109873>.
- [66] Amiri MM, Shadman M, Estefen SF. A review of physical and numerical modeling techniques for horizontal-axis wind turbine wakes. *Renewable and Sustainable Energy Reviews* 2024;193:114279. <https://doi.org/10.1016/J.RSER.2024.114279>.
- [67] Shami TM, El-Saleh AA, Alswaitti M, Al-Tashi Q, Summakieh MA, Mirjalili S. Particle Swarm Optimization: A Comprehensive Survey. *IEEE Access* 2022;10:10031–61. <https://doi.org/10.1109/ACCESS.2022.3142859>.
- [68] Jain M, Saihpal V, Singh N, Singh SB. An Overview of Variants and Advancements of PSO Algorithm. *Applied Sciences* 2022, Vol 12, Page 8392 2022;12:8392. <https://doi.org/10.3390/APP12178392>.
- [69] Chiang, T.-A.; Che, Z.-H.; Hung, C.-W. A K-Means Clustering and the Prim's Minimum Spanning Tree-Based Optimal Picking-List Consolidation and Assignment Methodology for Achieving the Sustainable Warehouse Operations. *Sustainability* **2023**, *15*, 3544.